Applied Catalysis B: Environmental 219 (2017) 249–258

Contents lists available at ScienceDirect

Applied Catalysis B: Environmental

journal homepage: www.elsevier.com/locate/apcatb

Solvothermal synthesis of I-deficient BiOI thin film with distinct photocatalytic activity and durability under simulated sunlight

Shuo Cui, Guoqiang Shan, Lingyan Zhu*

Key Laboratory of Pollution Processes and Environmental Criteria, Ministry of Education, Tianjin Key Laboratory of Environmental Remediation and Pollution Control, College of Environmental Science and Engineering, Nankai University, Tianjin, 300350, P.R. China

ARTICLE INFO

Article history:
Received 25 February 2017
Received in revised form 19 June 2017
Accepted 10 July 2017
Available online 11 July 2017

Keywords:
BiOI thin film
I vacancy
Calcination
BPA
Durability

ABSTRACT

I-deficient BiOI thin film was prepared via a facile solvothermal approach assisted with a ([C_6Mim]I) ionic liquid and calcination. The glass plates were pretreated with high pressurized water to make the substrate surface rough. A thin layer of BiOI grew stably on the rough surface of glass substrate with uniformly assembled nanosheets. As the preparation process repeated, BiOI crystals continued to grow and the film became denser and thicker with larger surface area and pore volume. During calcination, a small portion of iodine was lost and iodine vacancies formed, leading to I-deficient BiOI. The produced iodine vacancies acted as traps for photogenerated holes. Consequently, the recombination of photogenerated electrons and holes were significantly inhibited. The film displayed an excellent photoelectric property and distinct photocatalytic degradation efficiency for bisphenol A (BPA), a typical endocrine disrupting compound (EDC), under simulated sunlight. The film also displayed very good durability and reusability. Without necessity to separate the photocatalysts from reaction solution, the as-prepared I-deficient BiOI thin film displayed a great potential for practical wastewater treatment.

1. Introduction

Environmental pollution and energy crisis are two of the major problems encountered by human society [1]. Phototcatalysis driven by solar light has received intensive attentions because it shows great potential to be applied in the degradation of various environmental contaminants by efficiently utilizing natural solar energy [2]. Bismuth oxyhalides (BiOX, X = Cl [3], Br [4] and I [5]) are a family of visible light driven photocatalysts. They have extraordinary layered structure composed of $[Bi_2O_2]^{2+}$ layers and double layers of X^- anions [6]. The internal electric field between the positive $[Bi_2O_2]^{2+}$ layers and negative X^- layers favors the separation of photogenerated electrons and holes, leading to a remarkable photocatalytic activity [7]. Among the BiOX family, BiOI shows the greatest absorption in the visible light region owing to its smallest band gap energy, which was estimated to be about 1.8 eV [8]. It has been used in the degradation of many organic pollutants, such as Rhodamine B [9], methyl orange [10], methylene blue [11], tetracycline [5], bisphenol A (BPA) [12] and so on. However, its photocatalytic activity still needs to be further improved for practical application. Thus, many studies made efforts to enhance the photocatalytic performance by doping (Ti [13], Ag [14], Fe [15], Au [16], carbon quantum dots [17] and so on) and coupling (graphene oxide [18], Ag_3PO_4 [19], ZnO [20], Fe_2O_3 [21] and so on). Most of them introduce foreign substances, which may bring undesirable thermal instability of the photocatalysts [22]. A modification without introducing foreign substances is desirable to improve the photocatalytic activity of BiOI.

In current application, photocatalysts are mainly used in the form of powders, which need to be separated from the solution after reaction using filtration or centrifugation [23–31]. This shortcoming restricts the extensive application of photocatalysts, and numerous studies tried to synthesize photocatalysts with magnetic property [32–34]. But this is usually at the expense of reduced photocatalytic activity [35,36]. In recent years, many efforts have been made to develop photocatalyst thin film since it immobilizes photocatalysts on a substrate and does not need separation process [37–39]. At present, numerous methods were used to prepare photocatalytic films, such as chemical vapor deposition (CVD) [40–42], physical vapor deposition (PVD) [43,44], sol-gel method [45–47] and solvothermal method [48–50]. The CVD and PVD methods usually need vacuum system and expensive equipment. Sol-gel

* Corresponding author at: The College of Environmental Science and Engineering, Nankai University, Tongyan Road 38, Tianjin 300350, China.
E-mail address: zhuly@nankai.edu.cn (L. Zhu).

http://dx.doi.org/10.1016/j.apcatb.2017.07.026
0926-3373/

method needs a strict control over reaction conditions to ensure catalysts adhere to substrates steadily [51]. Solvothermal synthesis, which does not need expensive equipment or complicated operations, always produces stable films under high temperature and high pressure [52].

A variety of BiOI composite films were synthesized by introducing other materials to form a composite, such as BiOI/SiO_2 [51], BiOI/BiBr [53], BiOI/ZnO [54], Bi_2O_3/BiOI [55], TiO_2/BiOI [56] and Fe doped BiOI [15]. In previous studies [57–59], it was reported that I-deficient BiOI particle photocatalyst displayed much better photocatalytic activity than that of stoichiometric BiOI without introducing foreign substances. Thus, it is hypothesized that if an I-deficient BiOI thin film were fabricated, it would have advantages of easy recovery as well as high reactivity without introducing foreign substances, solving the two main problems in present application of photocatalytic materials.

The current study aimed to prepare an I-deficient BiOI thin film on glass substrate by solvothermal synthesis. The as-synthesized film was calcined at high temperatures, which were then comprehensively characterized by XRD, XPS, FESEM, FT-IR, UV-vis-DRS, BET and so on. The films were applied for degrading bisphenol A (BPA), which is a typical endocrine disrupting compound (EDC) [60] and is regulated or limited in many countries [61], under simulated solar light irradiation. The durability and reusability of the films were evaluated, and the degradation mechanism was also investigated.

2. Experimental

2.1. Materials and reagents

1-hexyl-3-methylimidazolium iodide ([C_6Mim]I) was purchased from Energy Chemical (Shanghai, China). $Bi(NO_3)_3{\cdot}5H_2O$ and KI were obtained from Guangfu Technology Development Co. Ltd. (Tianjin, China). Isopropanol, methyl alcohol and ethylene glycol were purchased from Concord Technology Co. Ltd. Benzoquinone was purchased from Sigma Aldrich. All the chemicals were used without further purification. Ordinary glass plates (60 mm × 20 mm × 1.5 mm) were purchased from Joyo Chemical Materials Co., Ltd.

2.2. Film photocatalyst preparation

2.2.1. Pretreatment of glass plates

The glass plates were cleaned with 1 M HCl, ethyl alcohol and deionized water consecutively and then put in a Teflon-lined stainless steel autoclave, in which deionized water was added until 80% of its volume was filled. The autoclave was heated at 180 °C in an oven for 12 h. After cooling down, the glass plates were washed with deionized water in an ultrasonic bath and dried at 80 °C.

2.2.2. Preparation of I-deficient BiOI thin film

As illustrated in Fig. S1, 0.12 g of $Bi(NO_3)_3{\cdot}5H_2O$ and 0.147 g of [C_6Min]I ionic liquid were mixed with 35 mL of isopropanol and 5 mL of ethylene glycol. The pretreated glass plate was immersed in the solution and leaned against the inner wall of the autoclave. The Teflon-lined stainless steel autoclave was heated in an oven at 160 °C for 12 h. Afterward, the glass plate was taken out and calcined in muffle furnace at 400 °C for 1 h, which was followed by cooling at room temperature. Photocatalysts formed on both sides of glass. The synthesized sample was labeled as BiOI-1.This synthesis procedure was repeated for several times, and the obtained products were labeled as BiOI-X, where X refers to the running number of the preparation process. For example, BiOI-3 refers to the product which was prepared for three times. For comparison, BiOI powder was also prepared following the same procedures as the I-deficient BiOI film but without the glass plates or calcination, which was labeled as BiOI-P. BiOI-C was the sample of BiOI-P after calcination.

2.3. Characterization of the as-prepared materials

The purity and crystallinity of the as-prepared materials were characterized by X-ray diffraction (XRD) on D/MAX 2500 V diffractometer (Rigaku, Japan) with monochromatized Cu Kα radiation under 40 KV and 100 mA and the scanning range was from 8° to 80°. The field emission scanning electron microscopy (FESEM, LEO, 1530 vp, Germany) was used to obtain the morphologies and microstructures of the materials. The X-ray photoelectron spectroscopy (XPS, Kratos Axis Ultra DLD) with monochromatized Al Kα X-ray as the excitation source was applied to study the compositions and chemical states of the elements. The surface areas were obtained using the Brunauer–Emmett–Teller (BET) method, and the average pore diameter was obtained from the sorption/desorption isotherms of N_2 using the Barrett-Joyner-Halenda (BJH) equation by surface area and porosimetry analyzer (TriStar 3000, Micromeritics, USA). FT-IR spectra were carried out on MAGNA-560 Nicolet. UV–vis diffuse reflectance spectra (DRS) of the samples were measured on a Hitachi U-3010 spectrometer, and the spectra were recorded in the range of 200–800 nm. The mass ratio of Bi and I was measured by X-ray fluorescence spectrometer (XRF, MagixPW2403).

Photoelectrochemical test was performed on a CHI 600D electrochemical system (Chenhua Instruments Co. Shanghai) in a conventional three electrodes system containing ITO/photocatalyst electrode as the working electrode, a Pt wire serving as the counter electrode and saturated calomel electrode and Ag/AgCl (saturated KCl) used as the reference electrode. A single-compartment quart cell was filled with 0.1 M Na_2SO_4, which was used as electrolyte. The photoresponses of the photocatalysts were measured at 0.0 V as visible light was switched on and off at intervals [62].

2.4. Photocatalytic experiment and BPA analysis

Photocatalytic experiments were conducted in a XPA-7 photochemical reactor (Xujiang Electromechanical plant, Nanjing, China) equipped with 12 quartz tubes surrounding 800 W xenon lamp as simulated sunlight. As shown in Fig. S2, the glass plate with I-deficient BiOI film was hung in the tube containing 40 mL of BPA (10 mg/L). For comparison, 20 mg of the powder scraped from the glass substrate or 20 mg of BiOI-P was added in the tube containing 40 mL of BPA (10 mg/L). Before illumination, the solution was stirred for 1 h in dark to establish the adsorption-desorption equilibrium of BPA on the catalysts. An aliquot of 1 mL of the reaction solution was sampled at certain intervals and centrifuged at 8000 rpm. The supernatant was withdrawn and analyzed by high performance liquid chromatography (HPLC). Previous studies [63,64] reported that nitrotetrazolium blue chloride (NBT), which exhibited an absorption maximum at 259 nm, was used to determine the presence of $O_2^{\bullet-}$. NBT solution (1×10^{-5} mol/L) was prepared and the BiOI-5 film was hung in 40 mL of NBT solution. Similar to the degradation experiment, an 800 W xenon lamp was used to simulate sunlight and illuminate the film and solution. An aliquot of 5 mL of the reaction solution was sampled at certain intervals and centrifuged at 8000 rpm. The supernatant was withdrawn and the absorbance was measured by an Agilent Cary series UV–vis Spectrophotometer. To evaluate the reusability of the film, it was taken out from the reaction solution and washed with deionized water, which was followed by heating at 80 °C in oven. The film was then used for subsequent photodegradation, and this procedure was repeated several times.

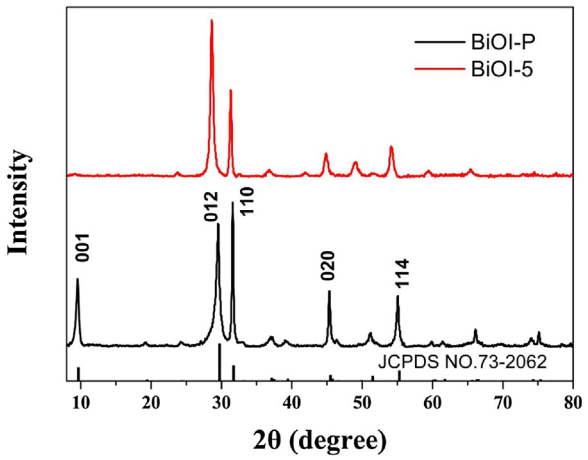

Fig. 1. The XRD patterns of BiOI-P and BiOI-5.

The BPA concentration was measured on a HPLC (Agilent 1260 infinity, Agilent Corporation, USA) with Fluorescence Detector (with emission wavelength at 220 nm and excitation wavelength at 350 nm) and equipped with an Agilent Eclipse XDB-C18 column (particle size 5 μm, 150 mm × 4.6 nm). The mobile-phase consisted of 65% methanol and 35% water at a flow rate of 0.15 mL/min. The column temperature was kept at 35 °C and injection volume was 100 μL.

3. Results and discussion

3.1. Characterization of the I-deficient BiOI film photocatalysts

Fig. 1 illustrates the X-ray diffraction (XRD) patterns of BiOI-5 and BiOI-P. Both samples were in good crystallinity. The diffraction peaks of BiOI-P could be indexed to tetragonal BiOI (JCPDS NO. 73-2062). No other residual phases were detected. Compared to BiOI-P, the diffraction peak {001} of BiOI-5 almost disappeared and other peaks shifted marginally to lower diffraction angles. This could be due to the process of calcination. When BiOI was calcined, the content of iodine element could decrease due to volatilization at high temperature. The concentrated bismuth and oxygen elements in the $[Bi_2O_2]^{2+}$ lattice might cause expansion and distortion of BiOI crystal structure [57,65].

Table 1
The relative atomic ratio in BiOI-P and BiOI-5.

Atom / Catalysts	Atom%			
	C1s	O1s	I3d	Bi4f
BiOI-P	42.82	29.69	10.69	16.81
BiOI-5	29.35	47.36	4.48	18.81

To investigate the purity of the I-deficient BiOI films and the valence states of the elements, XPS was carried out and the spectra are displayed in Fig. 2. There is no other element besides Bi, I, O and C. The spectrum of C 1 s was from the adventitious hydrocarbon in the XPS instrument itself, indicating that impurities were negligible in the prepared film. The two peaks of Bi elements at ~159 eV and ~164.4 eV could be assigned to Bi $4f_{7/2}$ and Bi $4f_{5/2}$, respectively [58]. The peaks at 530 eV and 531.6 eV are characteristic of a bismuth-oxygen in BiOX (X = Cl, Br and I) and H_2O or OH^- adsorbed on the surface of the photocatalyst, respectively. The peaks with binding energies of 629.4 eV and 617.8 eV are corresponding to the spin orbital doublets of I 3d (I $3d_{3/2}$ and I $3d_{3/5}$) [66]. In comparison to BiOI-P, the Bi 4f peaks of BiOI-5 shifted to a higher energy. It could be explained that during calcination, a portion of I atoms were replaced by O atoms. As a result, the interaction between Bi^{3+} and O^{2-} increased [67]. The relative atomic ratio obtained from XPS test indicated that the content of I in BiOI-5 did reduce, while that of O increased (Table 1), which is in agreement with the XRD results. In addition, the mass ratio of Bi and I was measured and the results were listed in Table 2. The atomic ratio of Bi/I decreased from 1.5 for BiOI-P to 4.6 for BiOI-5, confirming that a part of iodine atoms were

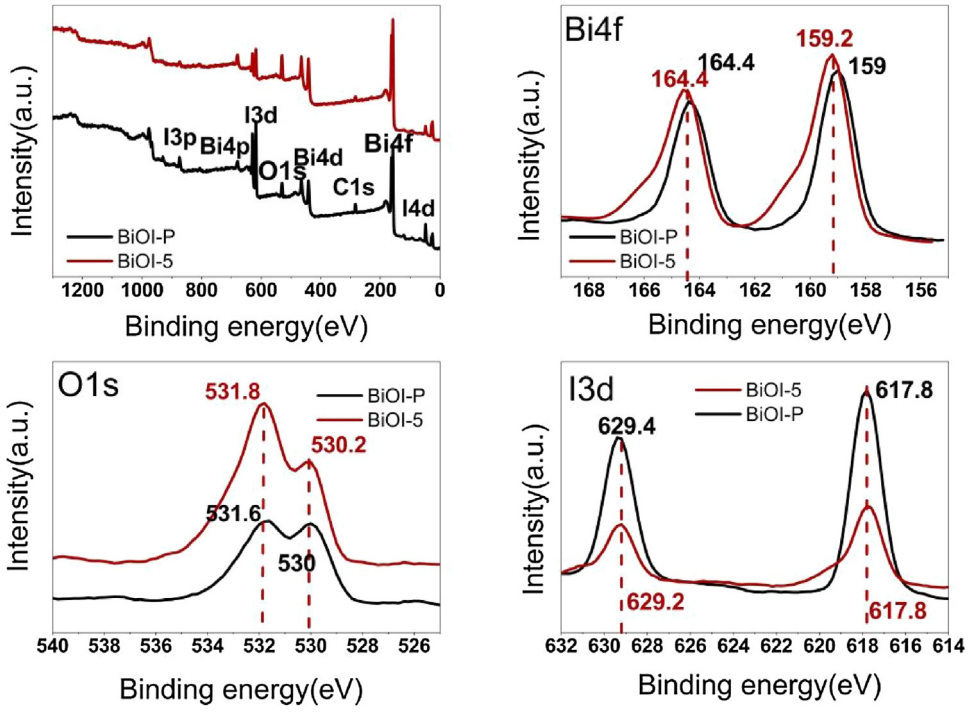

Fig. 2. The XPS results of BiOI-P and BiOI-5.

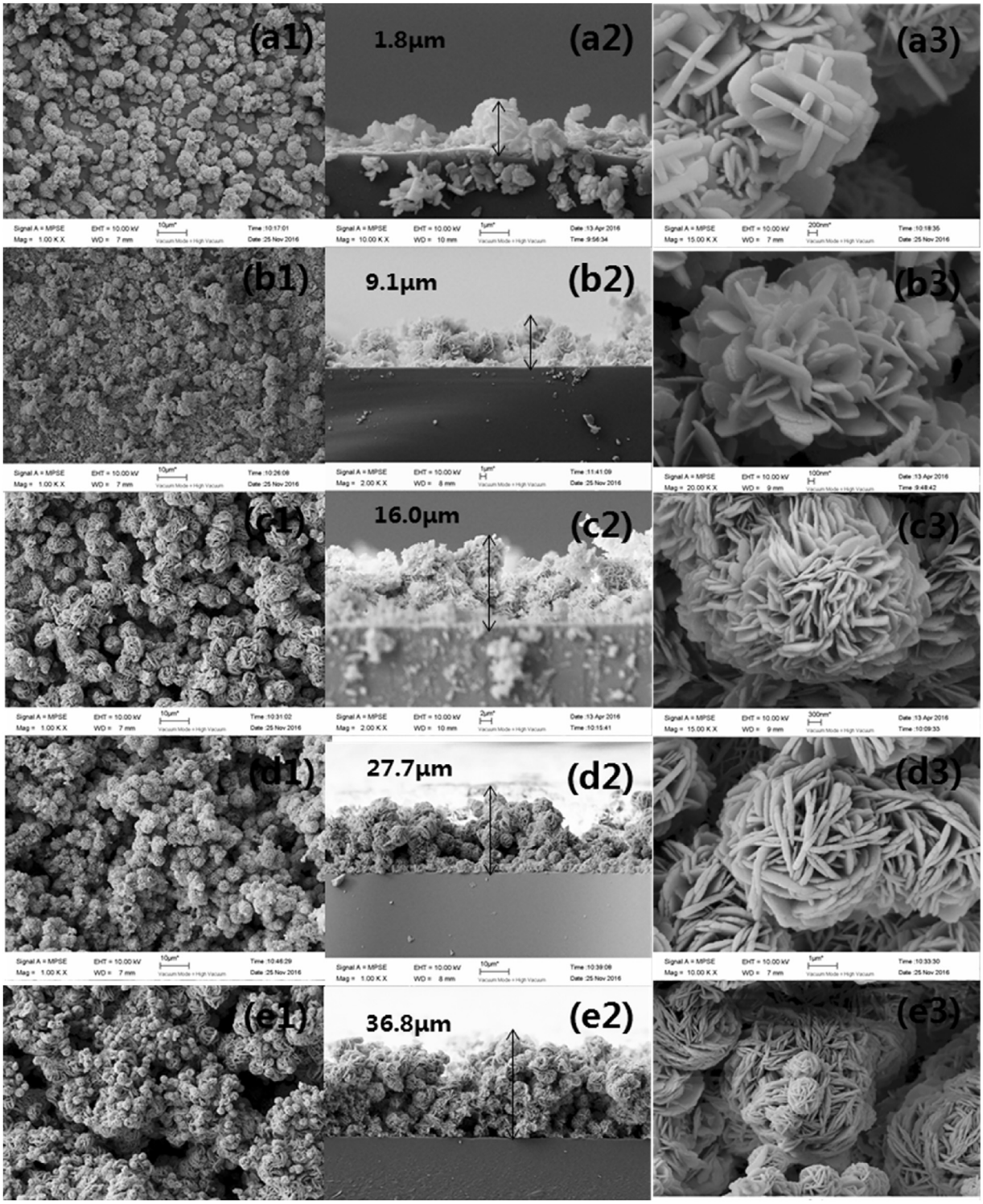

Fig. 3. The FESEM images of BiOI-1,2,3,4,5 films.

lost and abundant I vacancies were generated during calcination. This result agreed with previous reports [68,69].

The surface morphology of the glass plate was monitored by the field emission scanning electron microscope (FESEM). It was apparent in Fig. S3 that the surface of the glass substrates became rough and there were many indentations after high pressure water pretreatment. This change would be beneficial for steady growth of BiOI crystals on the glass substrate.

The surface nanostructures of the I-deficient BiOI films were characterized by FESEM and the results are exhibited in Fig. 3. Fig. 3a1–e1, a2–e2 and a3–e3 show the FESEM images of top view, side view and flower-like structure of BiOI-1 to BiOI-5, respectively. The as-synthesized I-deficient BiOI films were present as 3D flower-like structures which were assembled with nanosheets. With the increase of the runs of the synthesis processes, more and more catalysts grew on the substrate, while the nanosheets assembled more densely and the thickness increased. The mass of the catalysts grew

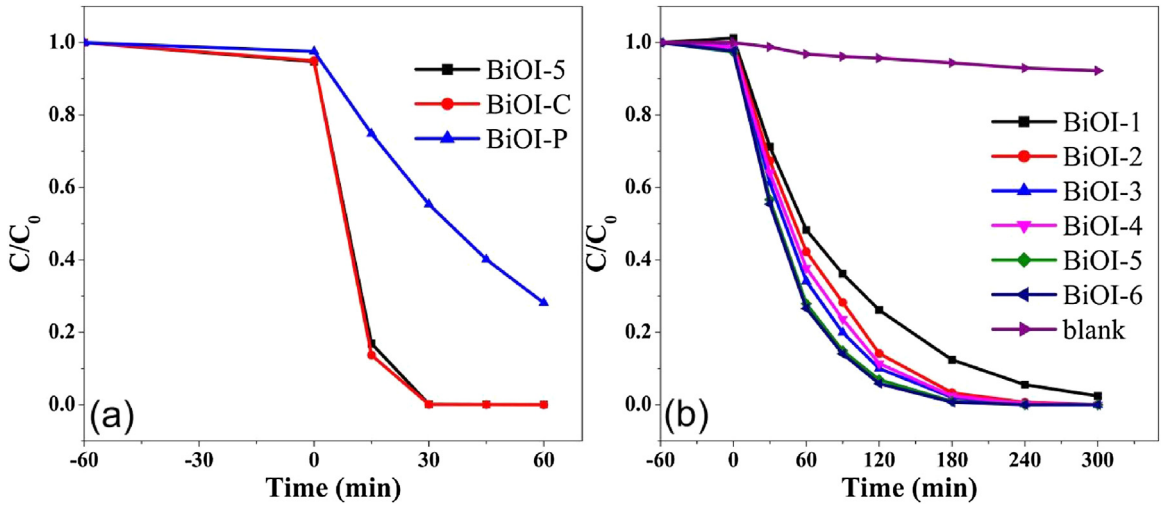

Fig. 4. (a) Photocatalytic degradation of BPA with BiOI-P powder and the powder scraped from BiOI-5; (b) degradation of BPA with BiOI-1 to BiOI-6.

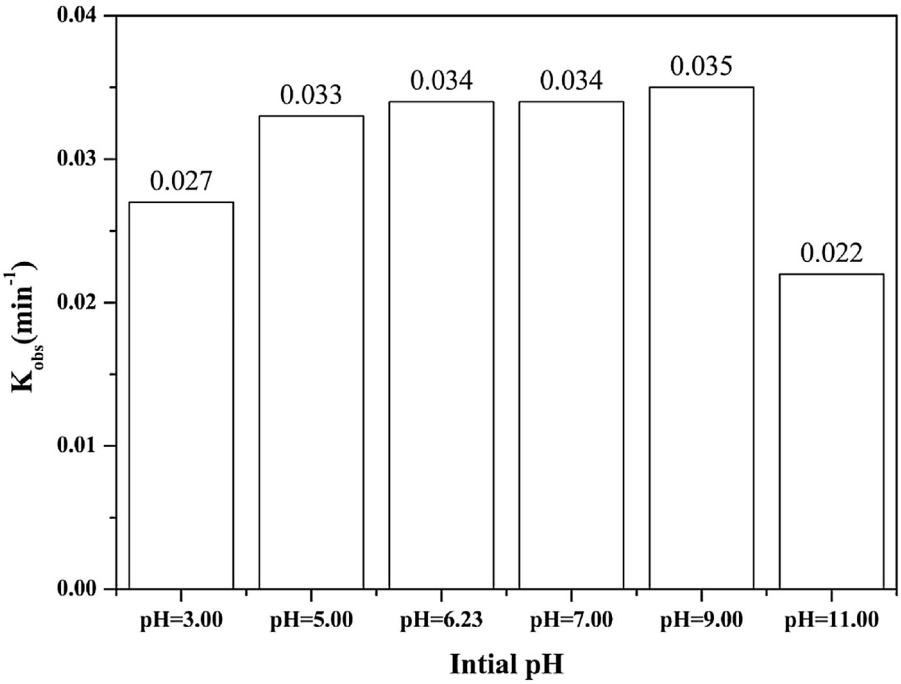

Fig. 5. The photocatalytic efficiency of BiOI-5 film under different initial pH values.

Table 2
Bismuth and iodine ratios for BiOI-P and BiOI-5 from XRF measurements.

Catalysts	BiOI-P		BiOI-5	
Elements	Bi	I	Bi	I
Weight percentage (%)	41.30	17.27	42.98	5.63
Atomic ratio (Bi/I)	1.5		4.6	

on the plates increased from 1.24 mg of BiOI-1 to 56.6 mg of BiOI-5. The increase of mass and degree of aggregation suggested that the content of active species and the specific surface area of the film increased, which would favor the photocatalytic reaction.

A BET test was carried out and the result (Fig. S4) indicated that there was a type IV loop with typical H3 hysteresis in the isotherms of BiOI-P and BiOI-5, indicating mesoporous structure of the prepared film photocatalysts. The BET surface areas of the BiOI-5 and the BiOI-P were 15.31 and 13.57 m^2/g, respectively. The BJH absorption cumulative volume of the pores increased from 0.047 to 0.055 cm^3/g after calcination. The increase of BET surface area and pore volume would supply more adsorption sites, thus promoting the photocatalytic activity.

Fig. S5 shows the result of FT-IR. It can be seen that the characteristic FT-IR peak of Bi—O—Si bond at 527 cm^{-1} was absent in glass and BiOI powders but was evidently present in the film products, indicating that there were Bi—O—Si bonds between the glass substrate and BiOI [70]. The chemical bonding might enhance the stability and reusability of the films.

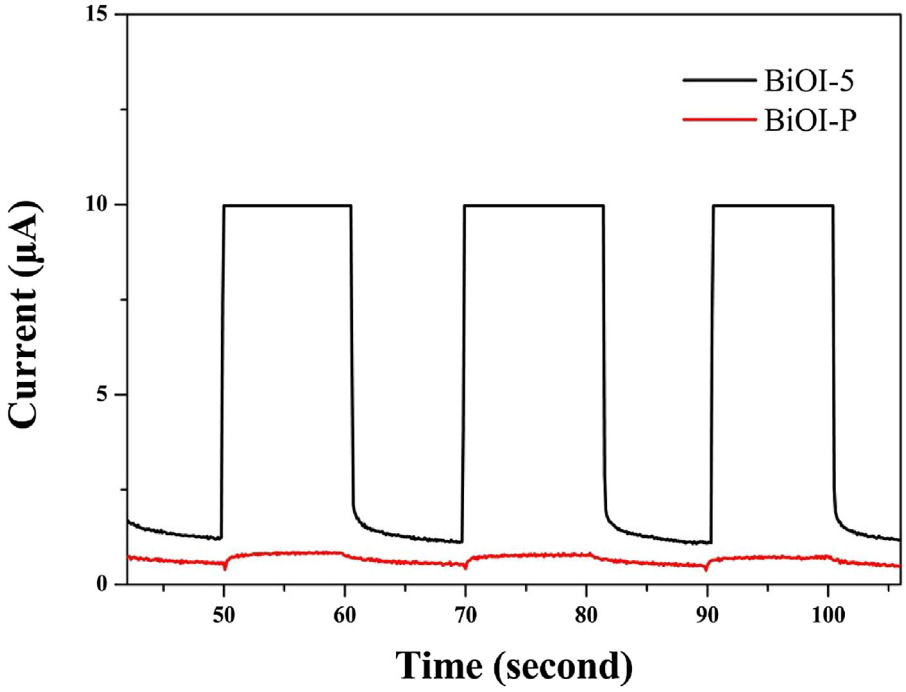

Fig. 6. Transient photocurrent responses of BiOI-P and BiOI-5.

3.2. Photocatalytic performance of the I-deficient BiOI films

Fig. 4(a) compares the photocatalytic degradation of BPA by BiOI-P, BiOI-C and the powders scraped from the BiOI-5 film. Both catalysts did not show significant adsorption capacity to BPA during the 60 min adsorption process. The degradation curves of BiOI-P and BiOI-C were almost the same, indicating that the interaction between photocatalysts and glass substrate did not affect photocatalytic activity. However, the photocatalytic activity of BiOI-5 was distinctly greater than that of BiOI-P. BPA was almost completely degraded in 30 min by I-deficient BiOI film while only 75% of BPA was degraded in 60 min by BiOI powder without calcination.

Fig. 4(b) compares the photocatalytic activities of the I-deficient BiOI films. With the increase of runs of synthesis process from 1 to 6, the photocatalytic activity increased, which could be due to the increased mass and surface area of the films. The performance of BiOI-6 was similar to that of BiOI-5. Hence BiOI-5 was selected for characterization and degradation tests.

Fig. 5 illustrates the impacts of solution pH on the photocatalytic performance of BiOI-5. The reaction constant was calculated using the following pseudo first-order kinetics equation: $-\ln(C_t/C_0) = K_{obs}t$, where the C_t and C_0 are the concentration of BPA at reaction time t and 0, respectively. K_{obs} is the pseudo-first-order rate constant and t is reaction time [71]. The regression coefficient R^2 was all greater than 0.95. As the pH increased from 3 to 9, the degradation rate increased gradually. As the pH further increased, the degradation efficiency decreased. The isoelectric point of BiOI-5 was estimated to be 4.16 (Fig. S6). When the initial pH was under 4.16, the surface potentials of BPA and BiOI-5 were positive and there was a repulsive interaction between them, leading to lower degradation efficiency. As the pH was in the range of 5–9, BPA is positively charged while the surface of BiOI-5 was negatively charged. Thus, there was an electrostatic attraction between them, which is beneficial for photocatalytic reaction. Nonetheless, when the pH increased over the dissociation constant pKa (9.6–11.2) of BPA, both BPA and BiOI-5 surface were negatively charged. A strong repulsion existed between them, leading to reduced degradation efficiency [72].

To explain the enhancement in photocatalytic activity of I-deficient BiOI films, UV–vis diffuse reflectance spectra (DRS) and photocurrent tests were conducted. The UV–vis DRS of BiOI-P and BiOI-5 are shown in Fig. S7 (a). Their absorption edges were at about 500 and 650 nm respectively. The band gaps of the catalysts were estimated using the following formula [73]: $\alpha hv = A(hv\text{-}E_g)^{n/2}$ where α, h, v and E_g represent absorption coefficient, Planck constant, photonic frequency and semi-conductor band gap energy, respectively, and A is a constant. As shown in Fig. S7 (b), the band gaps of BiOI-5 and BiOI-P were estimated to be 2.25 and 1.66 eV, which are close to those reported in previous studies [74,75].

Fig. 6 shows the photoelectric properties of the BiOI-5 and BiOI-P. The photocurrent of BiOI-5 was much higher than that of BiOI-P. As stated above, I element escaped from the BiOI crystals during calcination. Because the electronegativity of I element is lower than that of O element, the internal electric field in BiOI after calcination became stronger. The I-vacancies might act as hole traps, leading to an efficient separation of photoinduced electron-hole pairs and boosting its photoactivity [57]. This was the main reason accounting for the much higher photocatalytic activity of BiOI-5 than that of BiOI-P, although the photoabsorption of BiOI-5 was lower than that of BiOI-P. High separation efficiency of photoinduced electron-hole pairs was the main reason of distinct photocatalytic performance.

3.3. Photocatalytic mechanisms

Different kinds of scavengers (methyl alcohol as scavenger for $^{\bullet}OH$ [76], KI as scavenger for the h^+ [77], *p*-benzoquinone (BQ) as scavenger for $O_2^{\bullet-}$ [78]) were added in the reaction system to investigate which active species were responsible for the degradation of BPA. As shown in Fig. 7(a), degradation of BPA was not affected by the addition of methyl alcohol and KI, indicating that $^{\bullet}OH$ and holes were not the main active substances in the photocatalytic reaction. On the contrary, the degradation of BPA decreased distinctly when BQ was added. As shown in Fig. 8, the absorbance of

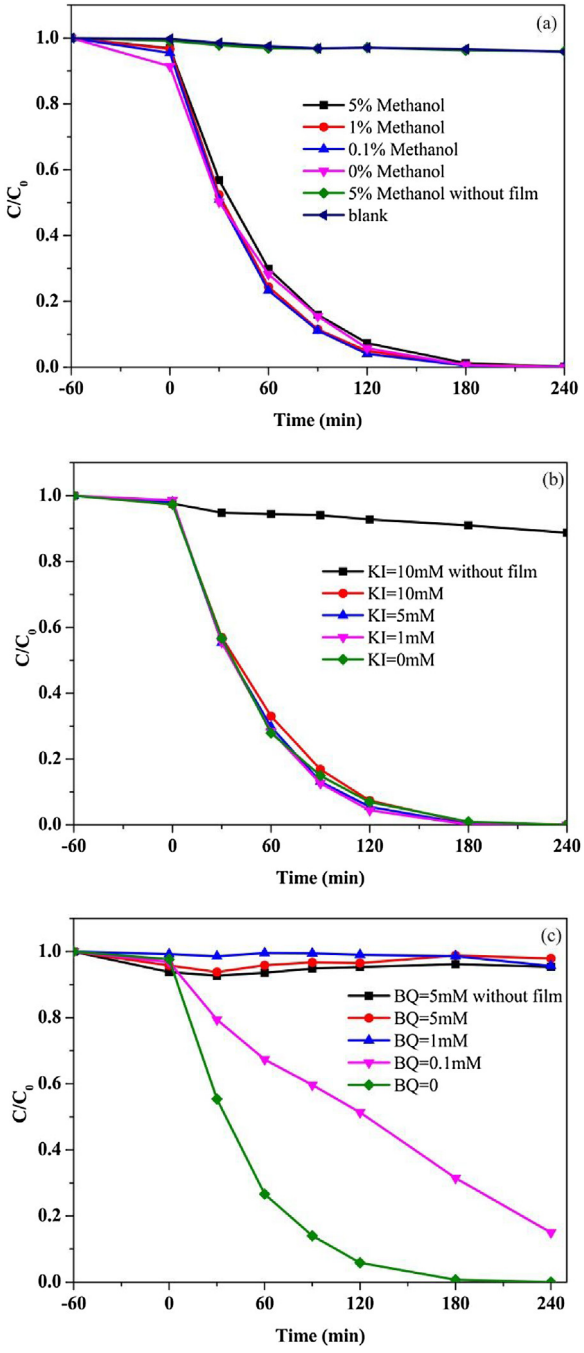

Fig. 7. Trapping experiments of reactive species: (a) methanol as quencher of •OH, (b) KI as quecher of h^+, and (c) BQ as quecher of $O_2^{\bullet -}$.

NBT decreased gradually as the reaction went on, confirming the present of $O_2^{\bullet -}$ [41]. Hence, $O_2^{\bullet -}$ could be the main active species for BPA degradation under simulated sunlight irradiation.

As the I-deficient BiOI film was irradiated with simulated sunlight, electrons on the VB were motivated up to CB [79]. Because the I-vacancies could act as a trap for the holes, the generated electrons displayed longer lifetime, which could efficiently react with O_2 to produce $O_2^{\bullet -}$. Subsequently, the $O_2^{\bullet -}$ attacked BPA and led to BPA degradation.

3.4. Reusability and stability

To investigate reusability and stability, the film was taken out of the reaction solution and washed with water. The film was reused for six times under the same reaction conditions and the result is shown in Fig. 9. The film displayed a great stability and maintained high photocatalytic activity after 6 cycles, suggesting that the as-prepared I-deficient BiOI films were very stable and displayed a great potential for reusability. Fig. 10 displays the XRD patterns of BiOI-5 before and after reactions. The XRD spectrum of BiOI-5 after 6 runs was almost the same as that of BiOI-5 before reaction, indicating excellent crystal stability of as-prepared film.

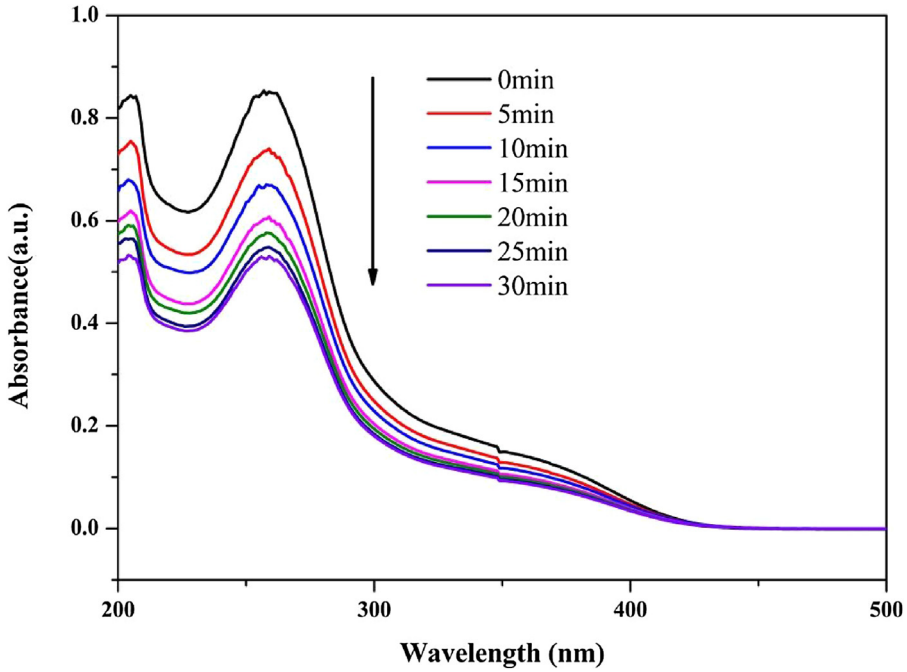

Fig. 8. Time-dependent absorption spectra of NBT for BiOI-5 under simulated light.

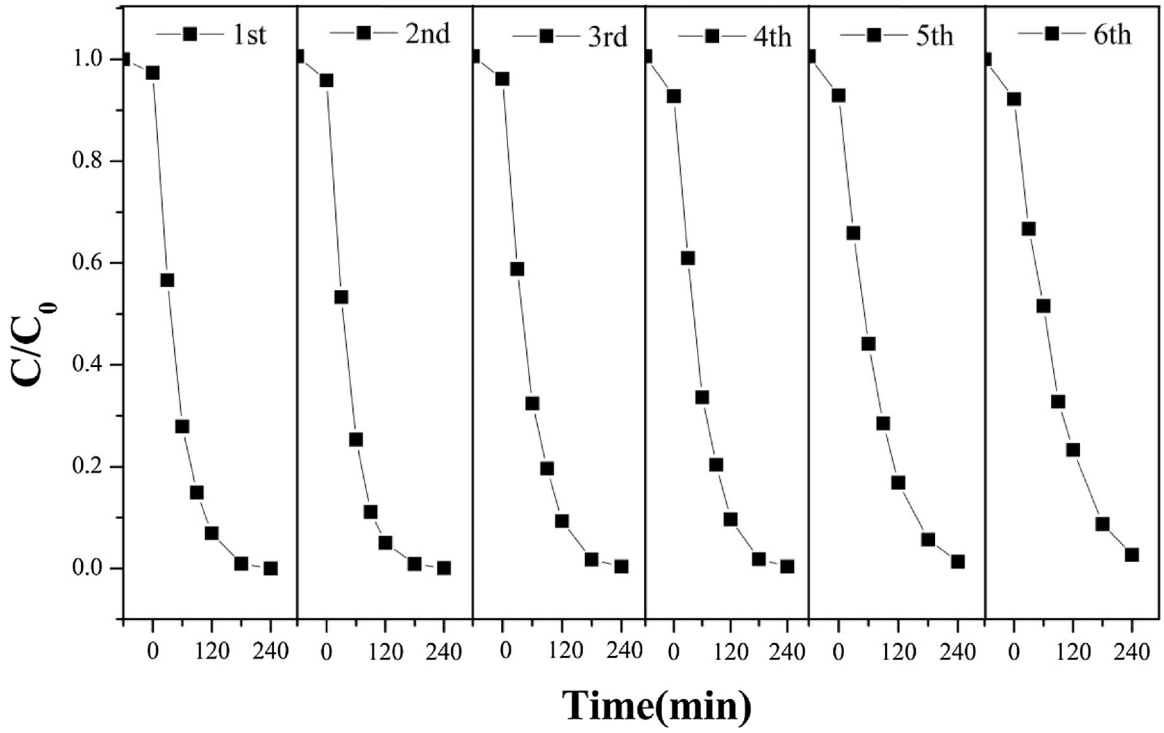

Fig. 9. Cycling test for the photocatalytic degradation of BPA.

4. Conclusions

I-deficient BiOI films with uniformly assembled nanosheets were prepared by a facile solvothermal approach assisted with calcination. During calcination, a portion of I elements escaped from the BiOI crystals, leading to enhanced internal electric field. As a result, the photogenerated electron-hole pairs were effectively separated, which greatly promoted the photocatalytic activities of the films. Furthermore, I-deficient BiOI was immobilized on the glass plates by Bi—O—Si bonds, making the film very stable and durable. Thus, the as-prepared I-deficient BiOI films displayed great photocatalytic activity and durability for the degradation of BPA under simulated sunlight and in a wide range of pH. Lots of energy could be saved since no separation of the catalyst from the reaction solution is necessary, and the film displayed great solar-light driven photocatalytic activity. Thus I-deficient BiOI films display a strong prospective for practical wastewater treatment.

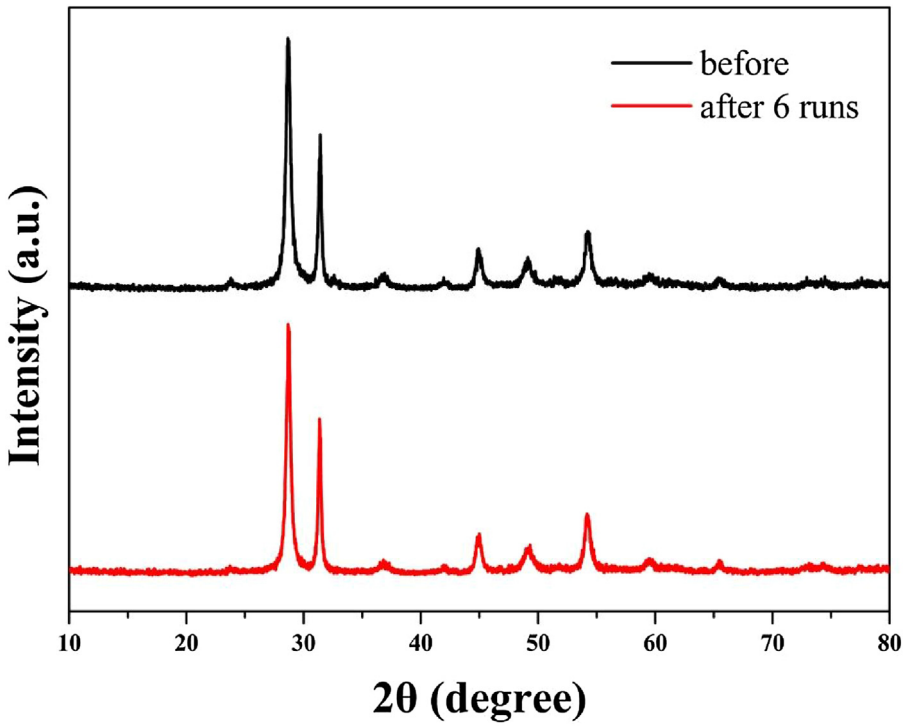

Fig. 10. The XRD patterns of BiOI-5 before and after reactions.

Acknowledgement

The authors gratefully acknowledge the financial support of Tianjin Municipal Science and Technology Commission (13JCZDJC35900), Ministry of Science and Technology (2014CB932001), and the Ministry of Education innovation team (IRT 13024).

Appendix A. Supplementary data

Supplementary data associated with this article can be found, in the online version, at http://dx.doi.org/10.1016/j.apcatb.2017.07.026.

The supporting data included the schematic of the preparation process of I-deficient BiOI film, reaction setup under simulated sunlight., FESEM images of the glass plate before treatment and after treatment, N_2 adsorption–desorption isotherms of prepared materials, FT-IR spectra of prepared materials, Zeta potential of BiOI-5 under different initial pH, UV-vis-DRS spectra of the prepared samples and plots of $(\alpha h\nu)^{1/2}$ versus energy.

References

[1] J.G. Hou, C. Yang, Z. Wang, S.Q. Jiao, H.M. Zhu, Appl. Catal. B Environ. 129 (2013) 333–341.
[2] Y.C. Liu, Y.J. Zhang, J. Math. Anal Appl. 393 (2012) 389–396.
[3] J.L. Hu, X. Wu, C.J. Huang, W.J. Fan, X.Q. Qiu, Appl. Surf. Sci. 387 (2016) 45–50.
[4] W.B. Li, Y.P. Zhang, Y.Y. Bu, Z.Y. Chen, J. Alloy. Compd. 680 (2016) 677–684.
[5] H.W. Huang, K. Xiao, Y. He, T. Zhang, F. Dong, X. Du, Y. Zhang, Appl. Catal. B Environ. 199 (2016) 75–86.
[6] M.E. Kazyrevich, M.V. Malashchonak, A.V. Mazanik, E.A. Streltsov, A.I. Kulak, C. Bhattacharya, Electrochim. Acta 190 (2016) 612–619.
[7] L.Q. Ye, Y.R. Su, X.L. Jin, H.Q. Xie, C. Zhang, Environ. Sci. Nano 1 (2014) 90–112.
[8] X.F. Chang, J. Huang, C. Cheng, Q. Sui, W. Sha, G.B. Ji, S.B. Deng, G. Yu, Catal. Commun. 11 (2010) 460–464.
[9] C.X. Liao, Z.J. Ma, X.F. Chen, X. He, J.R. Qiu, Appl. Surf. Sci. 387 (2016) 1247–1256.
[10] S.T. Huang, J.B. Zhong, J.Z. Li, J.F. Chen, Z. Xiang, M.J. Li, Q.C. Liao, Mater. Lett. 183 (2016) 248–250.
[11] Y. Long, Y. Wang, D. Zhang, P. Ju, Y. Sun, J. Colloid Interf. Sci. 481 (2016) 47–56.
[12] J. Di, J.X. Xia, S. Yin, H. Xu, L. Xu, Y.G. Xu, M.Q. He, H.M. Li, J. Mater. Chem. A 2 (2014) 5340–5351.
[13] J.L. Liang, J. Deng, M. Li, T.Y. Xu, M.P. Tong, Colloid. Surface. B 147 (2016) 307–314.
[14] N. Ekthammathat, S. Kidarn, A. Phuruangrat, S. Thongtem, T. Thongtem, Res. Chem. Intermediat. 42 (2016) 5559–5572.
[15] M.M. Wang, J.Z. Gao, G.Q. Zhu, N. Li, R.L. Zhu, X.M. Wei, P. Liu, Q.M. Guo, RSC Adv. 6 (2016) 106615–106624.
[16] C. Tang, L.F. Liu, Y.L. Li, Z.F. Bian, Appl. Catal. B Environ. 201 (2017) 41–47.
[17] J. Di, J.X. Xia, M.X. Ji, B. Wang, S. Yin, H. Xu, Z.G. Chen, H.M. Li, Langmuir 32 (2016) 2075–2084.
[18] R.G. He, S.W. Cao, D.P. Guo, B. Cheng, S. Wageh, A.A. Al-Ghamdi, J.G. Yu, Ceram. Int. 41 (2015) 3511–3517.
[19] Z.K. Cui, M.M. Si, Z. Zheng, L.W. Mi, W.J. Fa, H.M. Jia, Catal. Commun. 42 (2013) 121–124.
[20] J. Jiang, X. Zhang, P.B. Sun, L.Z. Zhang, J. Phys.Chem. C 115 (2011) 20555–20564.
[21] O. Mehraj, B.M. Pirzada, N.A. Mir, M.Z. Khan, S. Sabir, Appl. Surf. Sci. 387 (2016) 642–651.
[22] X. Ding, K. Zhao, L.Z. Zhang, Environ. Sci. Technol. 48 (2014) 5823–5831.
[23] K. Li, Y.P. Tang, Y.L. Xu, Y.L. Wang, Y.N. Huo, H.X. Li, J.P. Jia, Appl. Catal. B Environ. 140 (2013) 179–188.
[24] H.L. Lin, C.C. Zhou, J. Cao, S.F. Chen, Chin. Sci. Bull. 59 (2014) 3420–3426.
[25] H. Liu, W.R. Cao, Y. Su, Y. Wang, X.H. Wang, Appl. Catal. B Environ. 111 (2012) 271–279.
[26] X. Xiao, W.D. Zhang, J. Mater. Chem. A. 20 (2010) 5866–5870.
[27] M.N. Chong, B. Jin, C.W.K. Chow, C. Saint, Water Res. 44 (2010) 2997–3027.
[28] H.X. Qin, Y.Y. Bian, Y.X. Zhang, L.F. Liu, Z.F. Bian, Chin. J. Chem. 35 (2017) 203–208.
[29] Y.L. Li, Y.Y. Bian, H.X. Qin, Y.X. Zhang, Z.F. Bian, Appl. Catal. B Environ. 206 (2017) 293–299.
[30] Z.F. Bian, J. Zhu, H.X. Li, J. Photoch. Photobiol. A Rev. 28 (2016) 72–86.
[31] F.L. Cao, Y.L. Li, C. Tang, X.F. Qian, Z.F. Bian, Res Chem, Intermed 42 (2016) 5975–5981.
[32] X.C. Meng, Z.S. Zhang, J. Colloid Interf. Sci. 485 (2017) 296–307.
[33] M. Stefan, C. Leostean, O. Pana, D. Toloman, A. Popa, I. Perhaita, M. Senila, O. Marincas, L. Barbu-Tudoran, Appl. Surf. Sci. 390 (2016) 248–259.
[34] J.J. Ding, L.Z. Liu, J.J. Xue, Z.W. Zhou, G.Y. He, H.Q. Chen, J. Alloy. Compd. 688 (2016) 649–656.
[35] S.H. Xu, D.L. Feng, D.X. Li, W.F. Shangguan, Chin. J. Chem. 27 (2009) 610.
[36] X.W. Liu, Z. Fang, X.J. Zhang, W. Zhang, X.W. Wei, B.Y. Geng, Cryst. Growth Des. 9 (2009) 197–202.
[37] C.H. Hung, C. Yuan, H.W. Li, J. Hazard Mater. 322 (2017) 243–253.
[38] S.L. Lee, L.N. Ho, S.A. Ong, Y.S. Wong, C.H. Voon, W.F. Khalik, N.A. Yusoff, N. Nordin, Chemosphere 166 (2017) 118–125.
[39] S. Ramasundaram, M.G. Seid, J.W. Choe, E.J. Kim, Y.C. Chung, K. Cho, C. Lee, S.W. Hong, Chem. Eng. J. 306 (2016) 344–351.

[40] B.J. Starr, V.V. Tarabara, M. Herrera-Robledo, M. Zhou, S. Roualdes, A. Ayral, J. Membrane Sci. 520 (2016) 812–813.
[41] L.J. Ye, S.J. Chen, Appl. Surf. Sci. 389 (2016) 1076–1083.
[42] B. Blackburn, I. Hassan, C. Zhang, C. Blackman, K. Holt, C. Carmalt, J. Nanosci. Nanotechnol. 16 (2016) 10112–10116.
[43] B. Henkel, T. Neubert, S. Zabel, C. Lamprecht, C. Selhuber-Unkel, K. Raetzke, T. Strunskus, M. Vergoehl, F. Faupel, Appl. Catal. B Environ. 180 (2016) 362–371.
[44] Y.S. Ham, M.J. Kim, J. Choi, S. Choe, T. Lim, S.K. Kim, J.J. Kim, J. Nanosci. Nanotechnol. 16 (2016) 10846–10852.
[45] W.P. Hsu, M. Mishra, W.S. Liu, C.Y. Su, T.P. Perng, Appl. Catal. B Environ. 201 (2017) 511–517.
[46] M.A. Mohamed, W.N.W. Salleh, J. Jaafar, M.S. Rosmi, Z.A.M. Hir, M. Abd Mutalib, A.F. Ismail, M. Tanemura, Appl. Surf. Sci. 393 (2017) 46–59.
[47] P.P. Zhou, Z.G. Le, Y. Xie, J. Fang, J.W. Xu, J. Alloy. Compd. 692 (2017) 170–177.
[48] Z.S. Liu, B.T. Wu, J.N. Niu, X. Huang, Y.B. Zhu, Appl. Surf. Sci. 288 (2014) 369–372.
[49] P.F. Wang, Y.H. Ao, C. Wang, J. Hou, J. Qian, Mater. Lett. 101 (2013) 41–43.
[50] Y.M. Zhu, R.L. Wang, W.P. Zhang, H.Y. Ge, X.P. Wang, L. Li, Mater. Res. Bull. 61 (2015) 400–403.
[51] F. Shen, L. Zhou, J.J. Shi, M.Y. Xing, J.L. Zhang, RSC Adv. 5 (2015) 4918–4925.
[52] Y.N. Huo, R.J. Hou, X.F. Chen, H.B. Yin, Y. Gao, H.X. Li, J. Mater. Chem. A 3 (2015) 14801–14808.
[53] Z.S. Liu, H.S. Ran, B.T. Wu, P.Z. Feng, Y.B. Zhu, Colloid Surf. Aspects 452 (2014) 109–114.
[54] P.Y. Kuang, J.R. Ran, Z.Q. Liu, H.J. Wang, N. Li, Y.Z. Su, Y.G. Jin, S.Z. Qiao, Chem. Eur. J. 21 (2015) 15360–15368.
[55] Y.P. Cong, Y. Ji, Y.H. Ge, H. Jin, Y. Zhang, Q. Wang, Chem. Eng. J. 307 (2017) 572–582.
[56] J.Q. Liu, L.L. Ruan, S.B. Adeloju, Y.C. Wu, Dalton Tran. 43 (2014) 1706–1715.
[57] Y. Guan, S.M. Wang, X. Wang, C. Sun, Y.B. Wang, Z.Y. Ling, RSC Adv. 6 (2016) 2641–2650.
[58] X. Xiao, W.D. Zhang, RSC Adv. 1 (2011) 1099–1105.
[59] X. Xiao, C.L. Xing, G.P. He, X.X. Zuo, J.M. Nan, L.S. Wang, Appl. Catal. B Environ. 148 (2014) 154–163.
[60] W. Jiang, W.T. Li, F. Xiao, D.S. Wang, Z.C. Wang, Sep. Purif. Technol. 173 (2017) 244–249.
[61] H.B. Jin, L.Y. Zhu, Water Res. 103 (2016) 343–351.
[62] C. Chang, L.Y. Zhu, S.F. Wang, X.L. Chu, L.F. Yue, ACS Appl. Mater. Inter. 6 (2014) 5083–5093.
[63] Y. Yu, C.Y. Cao, H. Liu, P. Li, F.F. Wei, Y. Jiang, W.G. Song, J. Mater. Chem. A. 2 (2014) 1677–1681.
[64] L.Q. Ye, J.Y. Liu, Z. Jiang, T.Y. Peng, L. Zan, Nanoscale 5 (2013) 9391–9396.
[65] R.A. He, S.W. Cao, J.G. Yu, Y.C. Yang, Catal. Today 264 (2016) 221–228.
[66] Z.J. Zhao, F. Liu, L.Z. Zhao, S.K. Yan, Appl. Phys. A Mater. 103 (2011) 1059–1065.
[67] Y. Guan, S.M. Wang, X. Wang, C. Sun, Y.B. Wang, Z.Y. Ling, RSC Adv. 6 (2016) 2641–2650.
[68] M.C. Long, P.D. Hu, H.D. Wu, Y.Y. Chen, B.H. Tan, W.M. Cai, J. Mater. Chem. A 3 (2015) 5592–5598.
[69] M.C. Long, P.D. Hu, H.D. Wu, J. Cai, B.H. Tan, B.X. Zhou, Appl. Catal. B Environ. 184 (2016) 20–27.
[70] Y.Q. Jia, Y.X. Yang, Y.N. Guo, W. Guo, Q. Qin, X. Yang, Y.H. Guo, Dalton Tran. 44 (2015) 9439–9449.
[71] C. Chang, L.Y. Zhu, S.F. Wang, X.L. Chu, L.F. Yue, ACS Appl. Mat. Interfaces 6 (2014) 5083–5093.
[72] S.W. Gao, C.S. Guo, J.P. Lv, Q. Wang, Y. Zhang, S. Hou, J.F. Gao, J. Xu, Chem. Eng. J. 307 (2017) 1055–1065.
[73] M.A. Butler, J. Appl. Phys. 48 (1977) 1914.
[74] W.W. Lee, C.S. Lu, C.W. Chuang, Y.J. Chen, J.Y. Fu, C.W. Siao, C.C. Chen, RSC Adv. 5 (2015) 23450–23463.
[75] X.Y. Qin, H.F. Cheng, W.J. Wang, B.B. Huang, X.Y. Zhang, Y. Dai, Mater. Lett. 100 (2013) 285–288.
[76] R. Hazime, C. Ferronato, L. Fine, A. Salvador, F. Jaber, J.M. Chovelon, Appl. Catal. B Environ. 126 (2012) 90–99.
[77] E. Felis, S. Ledakowicz, J.S. Miller, Water Environ. Res. 83 (2011) 2154–2158.
[78] Y.K. Huang, S.F. Kang, Y. Yang, H.F. Qin, Z.J. Ni, S.J. Yang, X. Li, Appl. Catal. B Environ. 196 (2016) 89–99.
[79] L.Q. Ye, J.N. Chen, L.H. Tian, J.Y. Liu, T.Y. Peng, K.J. Deng, L. Zan, Appl. Catal. B Environ. 130 (2013) 1–7.